Climate Dynamics
https://doi.org/10.1007/s00382-018-4576-6

Robustness of the stratospheric pathway in linking the Barents-Kara Sea sea ice variability to the mid-latitude circulation in CMIP5 models

Bithi De[1,2] · **Yutian Wu**[2]

Received: 9 April 2018 / Accepted: 5 December 2018

Abstract
This study investigates the robustness of the stratospheric pathway in linking the sea ice variability over the Barents-Kara Sea in late autumn and early winter to the mid-latitude circulation in the subsequent winter. Two groups of models from the Coupled Model Intercomparison Project phase 5 (CMIP5) archive, one with a well-resolved stratosphere (high-top models) and the other with a poorly-resolved stratosphere (low-top models) are explored to distinguish the role of the stratospheric pathway. The results show that, collectively, high-top models are able to capture the persistent mid-latitude circulation response in the subsequent winter. The response in low-top models is, however, weaker and not as long-lasting most likely due to lack of stratospheric variability. Analysis of eddy heat flux reveals that stronger vertical wave propagation leads to a stronger response in stratospheric polar vortex in high-top models. In particular, it shows that zonal wave-2 eddy heat flux is crucial in leading to a stronger linear constructive interference with the climatological waves in high-top models. The results find that multi-model ensemble of CMIP5 high-top models is able to capture the prolonged impact of sea ice variability on the mid-latitude circulation and out performs the low-top models in this regard. Our study suggests that the representation of the stratosphere in climate models plays an important role in amplifying and extending the mid-latitude circulation response.

Keywords CMIP5 · Barents-Kara Sea sea ice variability · Troposphere–stratosphere coupling · Planetary scale waves

1 Introduction

The Arctic has experienced an unprecedented and accelerated sea ice loss and warming in the recent decades (Screen and Simmonds 2010), which is widely known as Arctic Amplification (AA). Global climate model simulations have projected a likelihood of further warming by the end of the current century with a doubling of near surface temperature increase over the Arctic compared to the global average (Collins and Coauthors 2013). The AA peaks in early winter possibly as a result of ice-albedo feedback with retreat of sea ice in the fall. However, contributions from enhanced atmospheric moisture and oceanic transport, cloud cover and longwave radiation feedback (e.g., Lu and Cai 2009; Collins and Coauthors 2013; Pithan and Mauritsen 2014; Cohen et al. 2014; Gong et al. 2017) are also important in shaping the emerging pattern.

It has been widely documented that sea ice variability, especially over the Barents and Kara Sea (BKS), could significantly alter the mid-latitude atmospheric circulation in the Northern Hemisphere (NH) (see review papers by Cohen et al. 2014; Barnes and Screen 2015, and references therein). A majority of the studies have detected a negative North Atlantic Oscillation (NAO) or Northern Annular Mode (NAM)-like pattern and a weakening of the stratospheric polar vortex as a result of sea ice loss. Nevertheless, considerable diversities still exist among the modeling studies (see a review paper by Screen et al. 2018) - some authors found a positive NAO-like pattern (Cassano et al. 2014; Screen et al. 2014) and a stronger polar vortex (Cai et al. 2012), while others suggested no significant impact on the NAO variability (Strey et al. 2010; Screen et al. 2013). In addition, from observations, autumn sea ice concentration (SIC)

Electronic supplementary material The online version of this article (https://doi.org/10.1007/s00382-018-4576-6) contains supplementary material, which is available to authorized users.

✉ Bithi De
bde@purdue.edu

[1] Department of Earth, Atmospheric, and Planetary Sciences, Purdue University, West Lafayette, IN, USA

[2] Lamont-Doherty Earth Observatory, Columbia University, Palisades, NY, USA

Published online: 12 December 2018

over the Arctic is found to precede the mid-latitude tropospheric circulation by about 2-4 motnhs (Wu and Zhang 2010). However, the dynamical mechanism that accounts for this prolonged remote impact of sea ice variability is not well understood. Previous studies (e.g., Kim et al. 2014; Sun et al. 2015; Wu and Smith 2016; Nakamura et al. 2016) have suggested that, in addition to the tropospheric pathway, the stratospheric pathway might also be potentially important in linking the late autumn early winter sea ice loss with the mid-latitude circulation via troposphere-stratosphere coupling, and therefore could probably explain the prolonged tropospheric circulation response (Zhang et al. 2017).

Similar to the mechanism that links October snow cover over Eurasia to mid-latitude winter (Smith et al. 2010; Cohen et al. 2010), recent studies have suggested that more planetary-scale waves, forced by reduced sea ice and enhanced warming in early winter, can propagate vertically into the stratosphere, increase the polar cap geopotential height and weaken the stratospheric polar vortex (Jaiser et al. 2013; Kim et al. 2014). The anomalous stratospheric circulation can persist for about 1–2 months and later descend into the troposphere, resulting in negative NAM-like pattern near the surface (Kim et al. 2014; Sun et al. 2015; Nakamura et al. 2016).

In particular, to explore the role of the stratosphere, Sun et al. (2015) performed a set of prescribed sea ice loss experiments using the Whole Atmosphere Community Climate Model version 4 (WACCM4), a high-top model with a well-resolved stratosphere, along with identical experiments using the Community Atmosphere Model version 4 (CAM4), the low-top counterpart with a poorly-resolved stratosphere developed at National Center for Atmospheric Research (NCAR). Both the high-top and low-top models have similar physics and horizontal resolution, however, they differ in vertical extent. In that study, statistically significant negative NAM-like response was found in the tropospheric circulation in late winter in WACCM4 with future projection of pan-Arctic sea ice decline while the response was much weaker in CAM4. Therefore, they suggested that the stronger circulation response in WACCM4 is likely due to the better representation of the stratosphere. Additionally, we note that most of the modeling studies that exhibit a negative NAO or a weakened polar vortex used high-top models with realistic simulation of the stratosphere (e.g. Wu and Smith 2016; Nakamura et al. 2016; Zhang et al. 2018). The studies that can not reproduce a tendency for the negative NAO or weakened polar vortex used low-top models with poorly represented stratosphere (Strey et al. 2010; Cai et al. 2012; Screen et al. 2013; Cassano et al. 2014).

Specifically, it has been proposed that the BKS SIC retreat could induce a long lasting effect on the tropospheric circulation through the stratospheric pathway (Nakamura et al. 2016; Zhang et al. 2017). However, so far, the remote effects of BKS SIC variability via troposphere-stratosphere coupling have been studied using single climate model simulations (Kim et al. 2014; Nakamura et al. 2016; Screen 2017; Zhang et al. 2017) and limited period of observations (Kim et al. 2014; Yang et al. 2016). Recently, it has been strongly advocated that simulations from diverse coupled models, using as many models as possible, are necessary to examine the robustness of the results (and references therin Screen et al. 2018). The Coupled Model Intercomparison Project phase 5 (CMIP5) experiments represent an excellent resource for multi-model study to assess the robustness of the stratospheric pathway, which has remained poorly explored in this regard. In this study, our goal is to revisit the prolonged impact of the BKS SIC variability and assess the robustness of the mechanism of the stratospheric linkage from diverse coupled model simulations. Moreover, our aim is to explicitly demonstrate the responses in planetary scale waves to SIC variability to better understand the troposphere-stratosphere coupling in multi-model ensemble settings.

Therefore, in this study, we shall use an ensemble of global climate models that participated in the CMIP5 experiments, focus on year-to-year variability and examine whether there is any significant difference between the high-top and low-top models. Earlier Charlton-Perez et al. (2013) documented that the stratospheric dynamical variability is under-represented in CMIP5 low-top models as compared to high-top models. Therefore, it is expected that differences can be seen between high-top and low-top models in their representation of the stratospheric pathway, i.e. the stratosphere-troposphere coupling that links the Arctic with the mid-latitudes. In this study, our key research questions include: 1. How well do CMIP5 models simulate the stratospheric pathway in linking the BKS SIC variability with the mid-latitude circulation? 2. Does the impact of BKS SIC variability differ between high-top and low-top models and what is the underlying mechanism?

Our study uniquely explores to what extent the circulation responses may be solely the result of BKS SIC variability via stratospheric pathway in the two groups of the models. The paper is organized as follows. Section 2 discusses about the CMIP5 model outputs and diagnostics. Section 3 describes the prolonged impact of BKS SIC variability on the mid-latitude circulation and surface air temperature and exploits the dynamics in high-top and low-top models. Section 4 concludes the paper.

2 Data and methods

2.1 Observations

ERA-Interim reanalysis data produced by the European Center for Medium-Range Weather Forecasts (ECMWF)

(Dee and Coauthors 2011) has been used to represent the atmospheric circulation in Figure S2. We use the monthly 700 hPa zonal wind in 1.5° longitude × 1.5° latitude horizontal resolution for the period of 1979–2014. In addition, we use monthly SIC derived from the passive microwave satellite data using bootstrap algorithm during the same time period. The SIC dataset is available in 448 × 304 horizontal (25 km mesh) grid in the NASA National Snow and Ice Data Center Distributed Active Archive Center (Comiso 2000). We focus on the year-to-year variability by removing the long-term linear trend from observations for all variables.

2.2 CMIP5 models

We analyze models with a well-resolved stratosphere (high-top models) and models with a poorly-resolved stratosphere (low-top models) in the CMIP5 pre-industrial control experiments (Taylor et al. 2012). The pre-industrial control experiments are forced with only natural forcings, i.e. solar radiation, natural aerosols and greenhouse gas concentrations that imitate the conditions prior to 1850 and do not have anthropogenic contributions, which would allow us to solely examine the impact of natural variability. In addition, significantly long span of model integrations in pre-industrial control experiments helps to improve the signal to noise ratio (Furtado et al. 2015). We select the models based on the availability of all variables, including monthly zonal and meridional wind, geopotential height and surface air temperature, and follow Charlton-Perez et al. (2013) to divide the models into high-top and low-top groups. The 10 high-top models are listed in Table 1 and the 10 low-top models are listed in Table 2. The two groups of models differ significantly in model top height and vertical resolution but not in horizontal resolution (as shown in Tables 1 and 2). We compare the average of the high-top and low-top models over the whole available time period.

2.3 Diagnostics

We focus on the late autumn and early winter SIC variability over the BKS region(70°–82°N, 15°–100°E), specifically during November and December (ND) following previous

Table 1 Horizontal resolution, model top height, vertical resolution and integration period of the high-top models from CMIP5 archive analyzed in this study

Number	Models	Resolution (lat × lon)	Lid heights (hPa)	Vertical levels	Time period (years)
1	CanESM2	2.7906° × 2.8125°	1	35	1096
2	CESM1-WACCM	1.88° × 2.5°	5.1×10^{-6}	66	200
3	GFDL-CM3	2° × 2.5°	0.01	48	500
4	HadGEM2-CC	1.25° × .875°	0.01	60	240
5	IPSL-CM5A-LR	1.8947° × 3.75°	0.04	39	1000
6	IPSL-CM5A-MR	1.2676° × 2.5°	0.04	39	300
7	MIROC-ESM	2.79° × 2.81°	0.0036	80	531
8	MIROC-ESMCHEM	2.79° × 2.81°	0.0036	80	255
9	MPI-ESM-LR	1.8653° × 1.875°	0.01	47	1000
10	MRI-CGCM3	1.12148° × 1.125°	0.01	48	500

Table 2 Horizontal resolution, model top height, vertical resolution and integration period of the low-top models from CMIP5 archive analyzed in this study

Number	Models	Resolution (lat × lon)	Lid heights (hPa)	Vertical levels	Time period (years)
1	bcc-csm1.1	2.7906° × 2.8125°	2.917	26	500
2	CCSM4	0.9424° × 1.25°	2.19	27	500
3	CNRM-CM5	1.4008° × 1.40625°	10	31	850
4	CSIRO-Mk3.6.0	1.86° × 1.87°	4.5	18	500
5	INM-CM4	1.5° × 2°	10	21	500
6	GFDL-ESM2M	2.02° × 2.5°	3	24	500
7	GFDL-ESM2G	2.02° × 2°	3	24	500
8	HadGEM2-ES	1.25° × 1.875°	3	38	239
9	MIROC5	1.4008° × 1.406°	3	40	200
10	NorESM1-M	1.8947° × 2.5°	3.54	26	501

studies (Kim et al. 2014; Yang et al. 2016; Zhang et al. 2017; Hoshi et al. 2017). We define BKS SIC index using the standardized SIC anomaly averaged during ND, area-averaged over the BKS region. Here we reverse the sign of the SIC index to emphasize the effect associated with sea ice loss. We perform lagged regression analysis between the BKS SIC index and winter time atmospheric variables to identify the possible impact of SIC loss on the atmospheric circulation in the subsequent months. We note that the variations of the monthly simulated BKS SIC among different models are comparable between the two groups and the models can approximately reproduce the observed detrended BKS SIC variability within the multi-model spread (Fig. S1). We find that the regression results remain robust while using October-November BKS SIC (not shown) instead of ND BKS SIC index.

In order to further diagnose the two-way troposphere-stratosphere coupling, we examine the variability of polar cap zonal mean zonal wind, area-averaged between 50°–70°N. In addition, we examine the zonal mean eddy heat flux $[v^*T^*]$ at 100 hPa to diagnose the upward wave propagation (Polvani and Waugh 2004; Simpson et al. 2009; Hoshi et al. 2017). Here, v and T are monthly meridional wind and air temperature, respectively, and the bracket and asterisk denote zonal mean and deviation from zonal mean, respectively.

We interpolate each model into a common grid of horizontal resolution of 2° longitude × 2° latitude to calculate multi-model mean. We estimate the agreement among models by examining if at least 80% of the models agree on the sign of the response. The statistical significance in observations is calculated using the students t-test at the 95% confidence level. We also find that the differences between the two groups of the models remain unchanged by varying the subsample of the models from the two groups (not shown). Additionally, we find that normalizing both the BKS SIC and the atmospheric variables does not change the conclusion (not shown).

3 Results

3.1 Prolonged response in tropospheric circulation

First, we examine the mid-latitude circulation response associated with BKS SIC variability in the observations (Fig. S2). The observations show a long-lasting impact of late autumn early winter SIC variability on the atmospheric circulation well into mid winter (January to March). Figure S2 shows the regression of observed detrended 700 hPa zonal wind onto the BKS SIC index from December to subsequent April. We find an equatorward shift of the tropospheric jet associated with a pronounced weakening on the poleward flank of the climatological jet. The signal is more pronounced over the North Atlantic-European sector from January to March and disappears in April. We note that the response in tropospheric jet, is not synchronized with the SIC variability, but rather maximizes in the subsequent January to March. Next we explore whether state-of-the-art coupled climate models can simulate the lead-lag relationship and whether there is any significant difference between high-top and low-top models.

Figure 1 shows the mid-latitude circulation response associated with BKS SIC variability in CMIP5 multi-model mean during February, as an example. The high-top models show a long-lasting impact that the atmospheric circulation associated with late autumn early winter SIC variability persists well into mid winter (February). Figure 1ab show the regression of 700 hPa zonal wind onto the BKS SIC during February, for two groups of models, respectively. We find a weakening on the poleward flank of the climatological jet for both groups. In addition, more importantly, the high-top multi-model mean (Fig. 1a), with well resolved stratosphere, shows a stronger weakening of the tropospheric jet over the North Atlantic-Europe sector, however, the deceleration of the tropospheric jet in this region in low-top multi-model mean (Fig. 1b) is much weaker. It is difficult to compare the model simulations with the observations due to the differences in the length of the time series and forcings, but the pattern of the high-top multi-model mean shows a closer resemblance to the observations, especially the jet weakening response over the North Atlantic sector (Fig. S2c), as compared to the low top multi-model mean.

In addition, we also show the regressed 500 hPa geopotential height field and find similar differences between the two groups of models (see Fig. 1c, d). A negative NAM-like pattern is seen with positive geopotential height anomaly over the Arctic and negative geopotential height anomaly over the North Atlantic region for both groups. However, high-top models (Fig. 1c) show a more pronounced geopotential height anomaly compared to low-top models (Fig. 1d), especially over the polar region of the North Atlantic sector. A similar negative NAM-like pattern is found in observations (e.g. Fig. 3C of Zhang et al. (2018)).

Previously, Furtado et al. (2015) studied the dynamical linkage between October snow cover over Eurasia and Arctic Oscillation (AO) in winter and found that CMIP5 models lack a robust lagged response compared to observations. Following Charney and Drazin (1961), they argued that the background zonal mean state in models may be responsible for the weaker propagation of the vertical component of wave activity flux that is proportional to the meridional heat flux and the subsequent stratospheric variability. It is possible that the circulation response can be sensitive to the basic state of the model (Kidston and Gerber 2010; Bader et al. 2011),

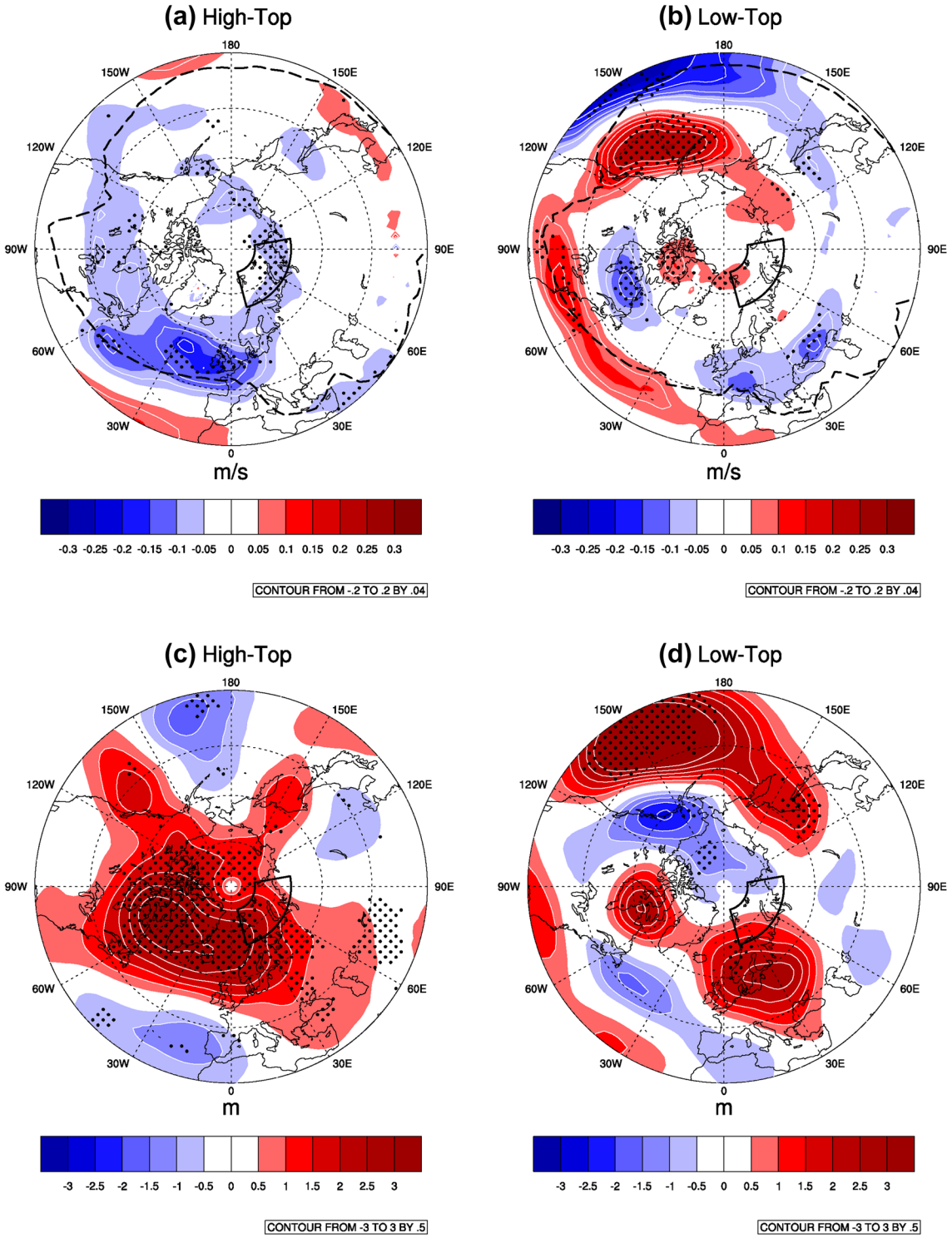

Fig. 1 Regression of 700 hPa zonal wind anomaly (in m/s per 1 standard deviation of BKS SIC loss) during February on the normalized BKS SIC variability in the previous November and December in **a** high-top models and **b** low-top models (color shadings and white contours with contour interval of 0.04 m/s), respectively. The dashed black line indicates the climatological jet position. The BKS region is highlighted in thick black box. The dots imply that at least 80% of the models agree on sign of change. **c**, **d** Are similar to **a**, **b** but for 500 hPa geopotential height (color shadings and white contour with contour interval of 0.5 m) during February in lower panel

which can result in high-top and low-top differences. For example, Kidston and Gerber (2010) mentioned that an equatorward bias in climatological jet-position can result in enhanced poleward shift of the jet. Therefore, here we examine whether differences in climatological jet latitude and jet speed in models affect the anomalous zonal wind over the North Atlantic and the inter-model spread. We define the jet response as the change of jet speed over the region (45°–90°N and 315°–360°E) with the strongest weakening of the jet in the North Atlantic sector. To calculate climatological jet statistics, we zonally average the 700 hPa zonal wind over the North Atlantic sector (45°–90°N and 270°–360°E), interpolate into a finer latitudinal grid of 0.05° and define the maximum zonal wind speed as the jet speed and the corresponding latitude as the jet latitude. We find that neither group of models shows any significant correlation between the jet response and the climatological jet-latitude (Fig. S3a). Although, we find a moderate yet statistically insignificant negative correlation between the jet response and the climatological jet speed in low-top models which suggests that low-top models with a faster climatological jet are more likely to produce a larger slowdown of the jet speed to sea ice variability (Fig. S3b). However, lack of robustness in this relationship is in contrast with the statistically robust circulation response as shown in Figure 1. Hence, we argue that the differences in circulation response between high-top and low-top models are not likely related to differences in climatology, but instead, are attributed to the representation of the stratospheric pathway (to be discussed next).

3.2 Dynamics of troposphere–stratosphere coupling

The previous section presented the differences between CMIP5 high-top and low-top models in simulating the impact associated with the BKS SIC variability on the midlatitude circulation. In this section, we attribute the differences between high-top and low-top models to the stratospheric pathway. Figure 2 shows the monthly evolution of polar cap zonal mean zonal wind from November to April associated with BKS SIC variability. We find that both groups of models simulate a weakening of the stratospheric polar vortex but with different strength. In the high-top multi-model mean, the weakening of the stratospheric polar vortex starts in December, maximizes in January at 10 hPa and gradually migrates downward reaching the lower troposphere in February (Fig. 2a). The downward descent of the stratospheric circulation response indicates possible stratosphere-troposphere coupling in mid-winter. However, in the low-top multi-model mean, the weakening of zonal wind is weaker and the tropospheric response is short-lived and disappears after January (Fig. 2b). Previously, Charlton-Perez et al. (2013) documented that the key reason behind short-lived tropospheric response in low-top models is the lack of stratospheric dynamical variability which results in reduced e-folding time scale of NAM-like signal.

To better understand the stronger weakening of the stratospheric polar vortex in high-top models compared to low-top models, we study the eddy heat flux at 100 hPa, which provides a diagnostic measurement of troposphere-stratosphere coupling (Polvani and Waugh 2004; Kim et al.

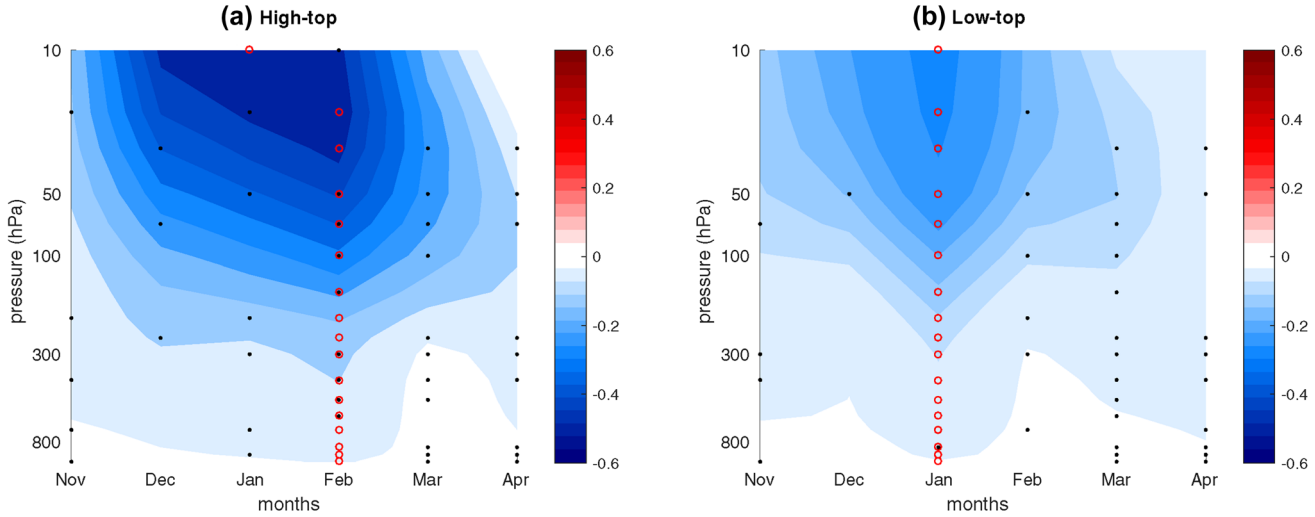

Fig. 2 Monthly evolution of zonal mean zonal wind (in m/s per 1 standard deviation of BKS SIC loss) averaged between 50°–70°N from November to April, associated with BKS SIC variability in November and December in **a** high-top models and **b** low-top models (color shadings). The red circles represent the months with minimum values at given pressure levels. The black dots indicate that at least 80% models agree on sign of change

2014; Sun et al. 2015). We choose December as the upward propagation phase, which is during the forcing period (ND) and coincides with the onset of the weakened polar vortex (Fig. 2). In the multi-model mean, an anomalous upward heat flux is seen in December in both high-top and low-top models (Fig. 3a, b). It primarily occurs in the vicinity of Eastern Eurasia (EE) region (50°–80°N, 140°–160°W) and Central Eurasia (CE) region (50°–80°N, 50°–90°E), which collocates with the climatological maxima of eddy heat flux. These two regions were also found as two important centers of action for linear constructive interference and troposphere-stratosphere coupling in Hoshi et al. (2017). Following an enhanced upward heat flux anomaly, the weakening of the stratospheric polar vortex reaches its maximum during January (Fig. 2). We closely compare this chain of events between the two groups of models, to explore the reason behind the stronger response in high-top models. In December, prior to the maximum stratospheric response in January, we find a stronger positive anomaly in eddy heat flux in the vicinity of CE and EE regions in high-top models (Fig. 3a) compared to low-top models (Fig. 3b), consistent with the more pronounced weakening of the stratospheric polar vortex in high-top models compared to low-top.

Further decomposition of 100 hPa eddy heat flux into zonal wave-1 and wave-2 components shows that the key difference between the two groups of models can be mainly attributed to wave-2 component (Fig. 3e, f) as the contributions from wave-1 component are almost identical (Fig. 3c, d). This results in stronger linear interference mechanism where the anomaly of wave-2 component is mostly in phase with the climatological wave and thus leads to larger upward wave-2 flux into the lower stratosphere in high-top models (Fig. 3e) (Garfinkel et al. 2010; Smith et al. 2010; Zhang et al. 2017). In contrast, for low-top models, the weaker response in wave-2 component results in reduced upward wave-2 flux into lower stratosphere from interference with climatological waves (Fig. 3f).

To further examine the wave propagation between the two groups, we study the wave-1 (Fig. 4) and wave-2 (Fig. 5) components of geopotential height at 500 hPa and at 50 hPa during upward propagation phase in December and during downward migration phase in February, respectively. In Fig. 2, we found that the downward descent of weakened zonal wind dies off after January in low-top models while the high-top models show long-lasting response up to February. Hence, we consider February as the downward migration phase to explicitly distinguish the persistence of stratosphere-troposphere coupling between the two groups. We choose two vertical levels to determine the phase tilt with height of the wave patterns and the wave propagation (following Shaw et al. 2014). We expect a west-ward phase tilt for troposphere-stratosphere coupling during upward wave propagation phase and an east-ward phase tilt for stratosphere-troposphere coupling during downward wave migration phase. In wave-1 component, for both groups, we find a west-ward phase tilt with height between the two vertical levels during December (Fig. 4a, b). However, in contrast to the high-top models (Fig. 4c), the low-top models do not show the east-ward phase tilt with height during February (Fig. 4d) which is an indication of no downward coupling. This is consistent with Fig. 2 where we find that the downward coupling disappears after January for low-top models. In contrast to wave-1, the wave-2 component (Fig. 5) shows a much weaker response and the two levels mostly overlap each other.

Therefore, the key difference between the two groups of models is a stronger stratospheric response due to stronger eddy heat flux and a longer-lived tropospheric signal following a stronger two-way coupling in high-top multi-model mean compared to low-top. However, as for why stratospheric wave propagation is distinct between the two groups of models, is beyond the scope of this study. As suggested in previous studies (Garfinkel et al. 2012; Sun et al. 2015), the weaker vertical wave propagation in low-top models could possibly be associated with a stronger polar vortex due to more wave reflection near the model lid (Sassi et al. 2010; Shaw and Perlwitz 2010; Sun et al. 2015). In addition, Shaw and Perlwitz (2010) found that different stratospheric states can also alter tropospheric wave climatology that may lead to different tropospheric wave interference in the two groups of models.

3.3 Missing mid-winter Eurasian cooling

Another possible consequence of SIC loss that has been discussed extensively in recent studies is the Eurasian cold air outbreaks. However, the evidence of the linkage between the Arctic and mid-latitude extremes is doubtful due to limited period of observations and poor understanding of how the dynamics works (e.g. see review papers by (Cohen et al. 2014; Shepherd 2016)). But several studies have suggested that a prominent warm Arctic cold Eurasia pattern (as found in Overland et al. 2011) is attributable to BKS SIC loss and an associated intensified Siberian high that advects cold air from the Arctic to the south (e.g. Mori et al. 2014; Vihma 2014; Kug et al. 2015).

In CMIP5 multi-model mean, however, the cold temperature anomaly over Eurasia during February is almost absent: there is a very small and statistically insignificant cold anomaly over Eurasia in high-top models (Fig. 6a) whereas the cold anomaly is absent in low-top models (Fig. 6b). We note that following previous discussions, here we focus on the prolonged Eurasian temperature response during February. Despite the missing Eurasian cooling in models during mid-winter, both high-top and low-top models can simulate

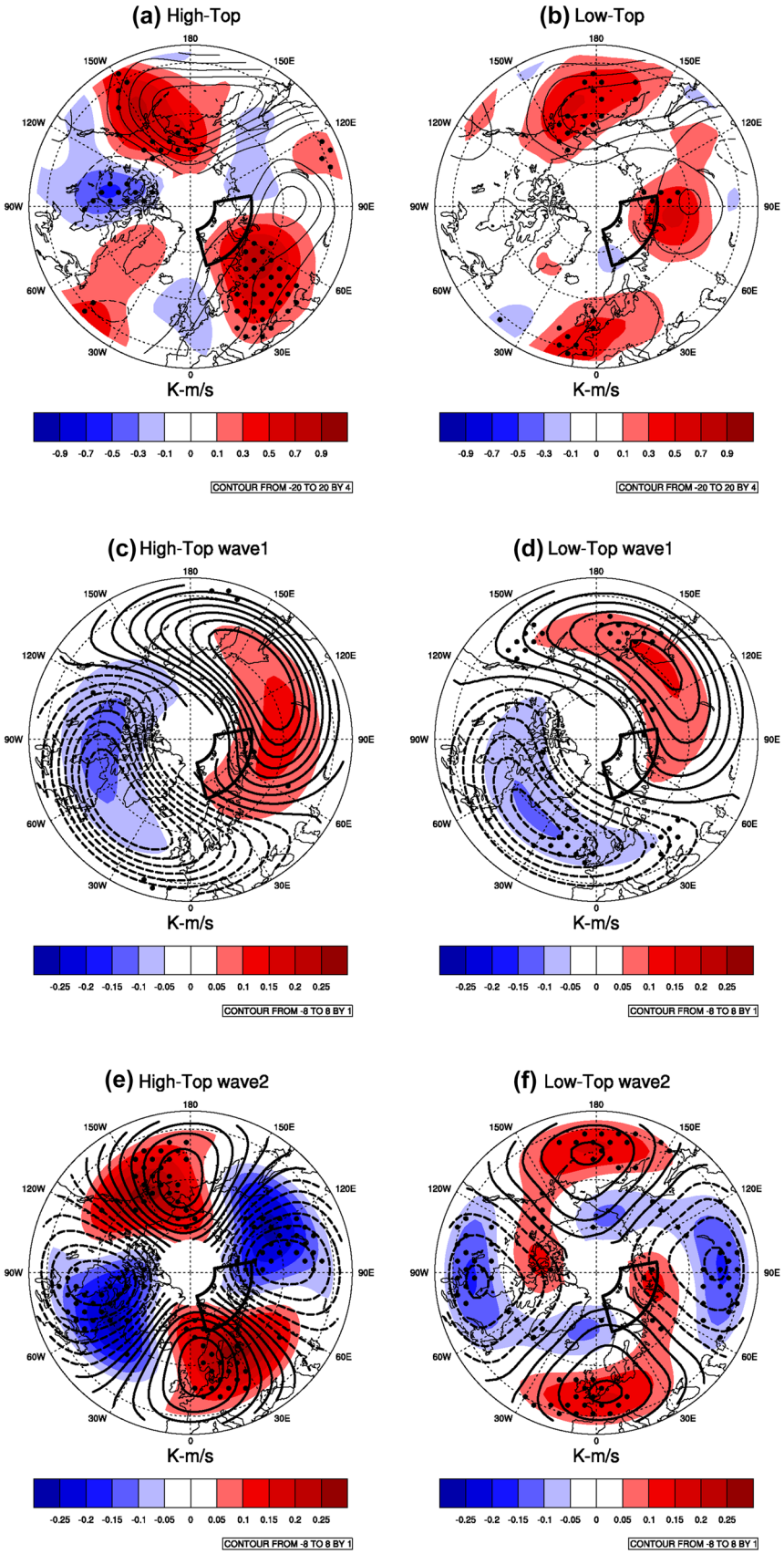

Fig. 3 Similar to Fig. 1 but for 100 hPa eddy heat flux (color shadings, in K m/s per 1 standard deviation of SIC loss) in December in **a** high-top models and **b** low-top models, respectively. The black contours (with a contour interval of 4 K m/s) indicate climatological poleward heat flux where positive values are solid while negative values are dashed. **c**–**f** are similar to **a** and **b** but for wave-1 and wave-2 100 hPa eddy heat flux response (color shadings), respectively. The black contours have an interval of 1 K m/s in **c**–**f**. Note different latitudinal extent compared to Fig. 1

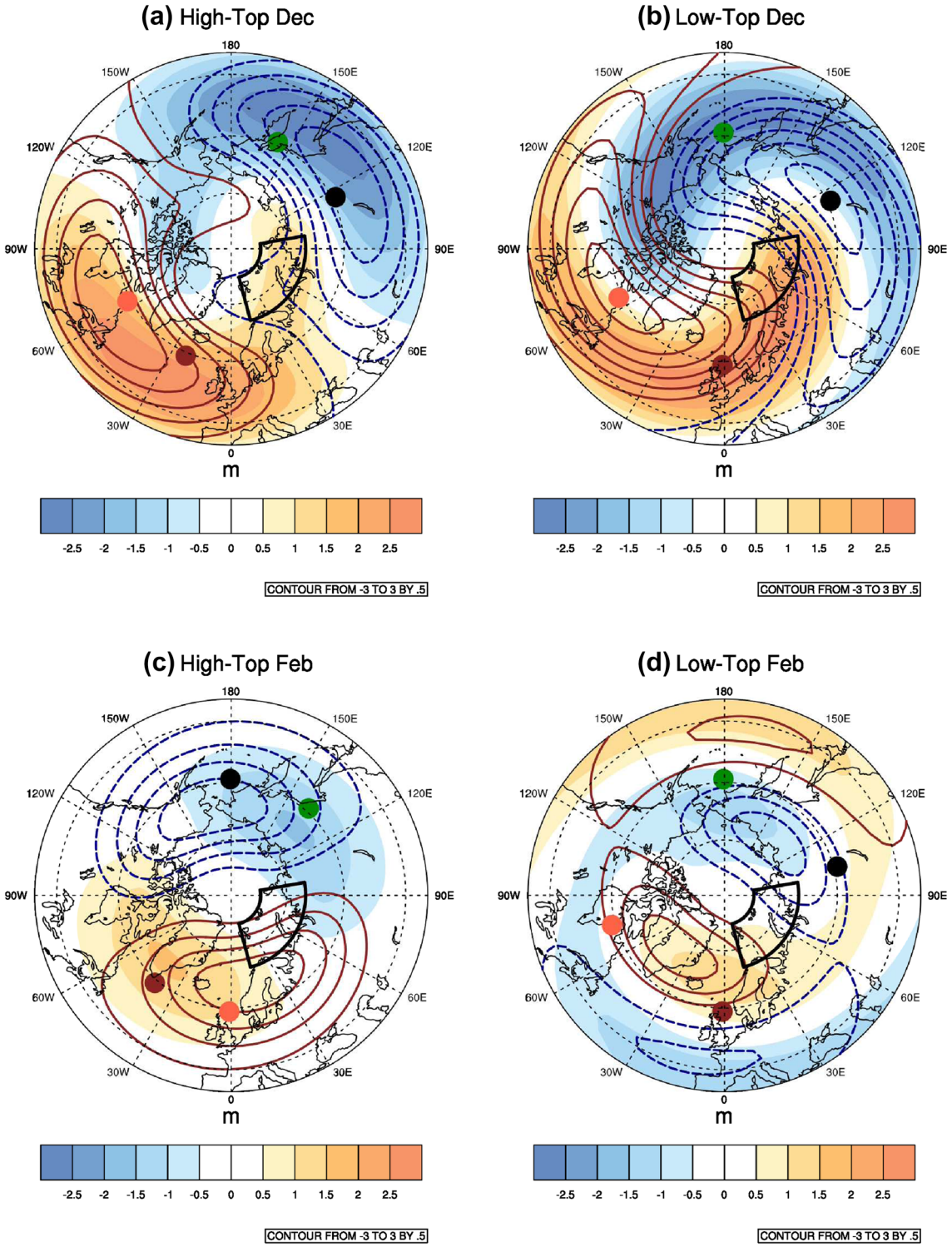

Fig. 4 Wave-1 geopotential height regression (per 1 standard deviation of BKS SIC loss) at 500 hPa (color shadings) and 50 hPa (contours) during December (**a**, **b**) and February (**c**, **d**), respectively. Contour interval is 0.5 m. Positive values in contours are solid brown while negative values are dashed blue and the zero contour is omitted. The solid brown dot and solid green dot represent the maxima and minima at 60°N, as an example, at 500 hPa. The solid light red dot and solid black dot represent the corresponding maxima and minima at 50 hPa, respectively. Note different latitudinal extent compared to Fig. 1

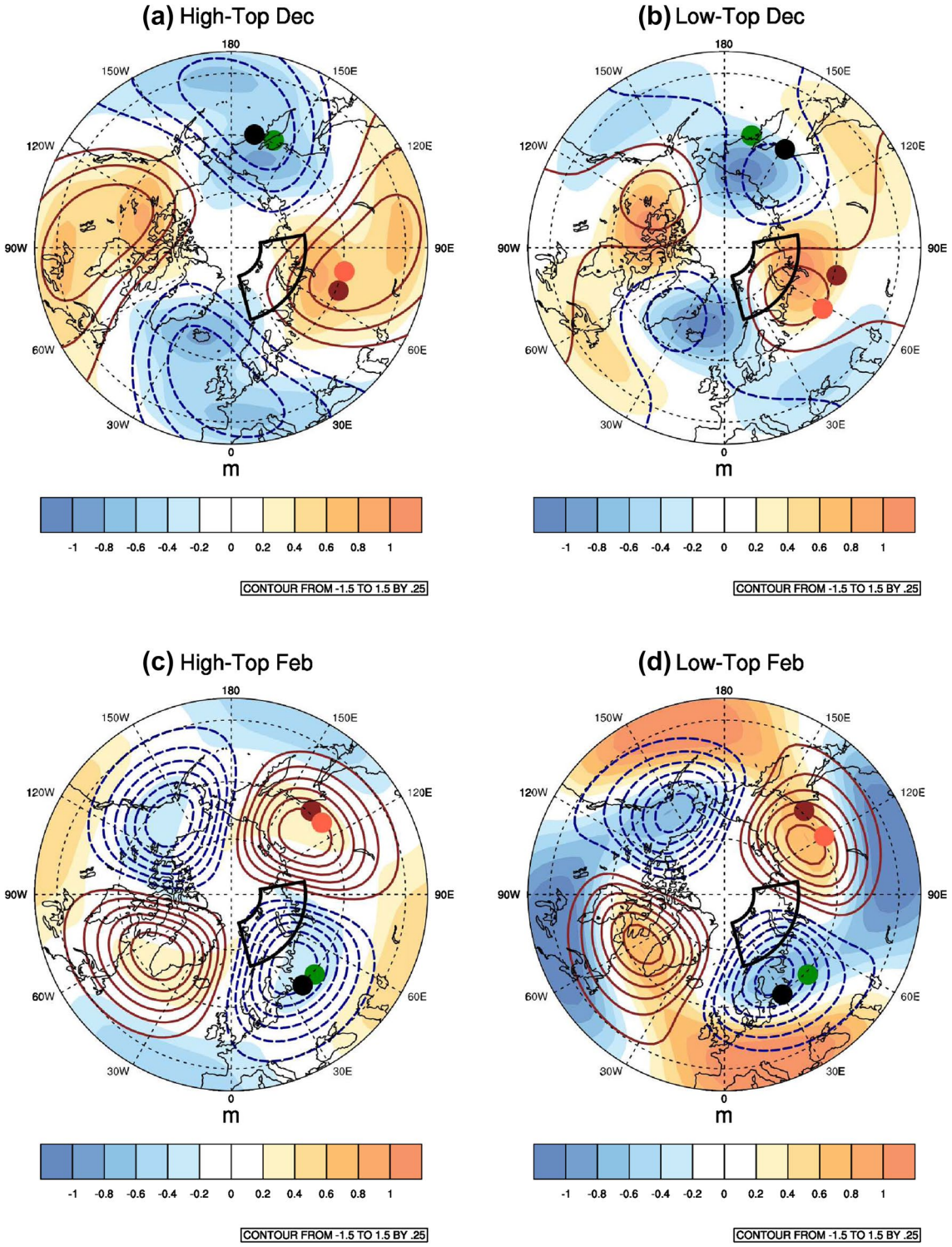

Fig. 5 Similar to Fig. 4 but for wave-2 geopotential height regression (in color shadings and black contours with contour interval of 0.25 m). Note the difference in colorbar from Fig. 4. Note different latitudinal extent compared to Fig. 1

the Eurasian cooling during early-winter (not shown), which possibly does not include a stratospheric pathway.

We argue, this is possibly due to inability of the models to simulate an intensified ridge near the Ural Mountains and a trough over Eastern Eurasia (Zhang et al. 2018). To further examine that, we investigate the relation between the mid-tropospheric circulation anomaly and Eurasian surface air temperature (SAT) anomaly among all the models. More

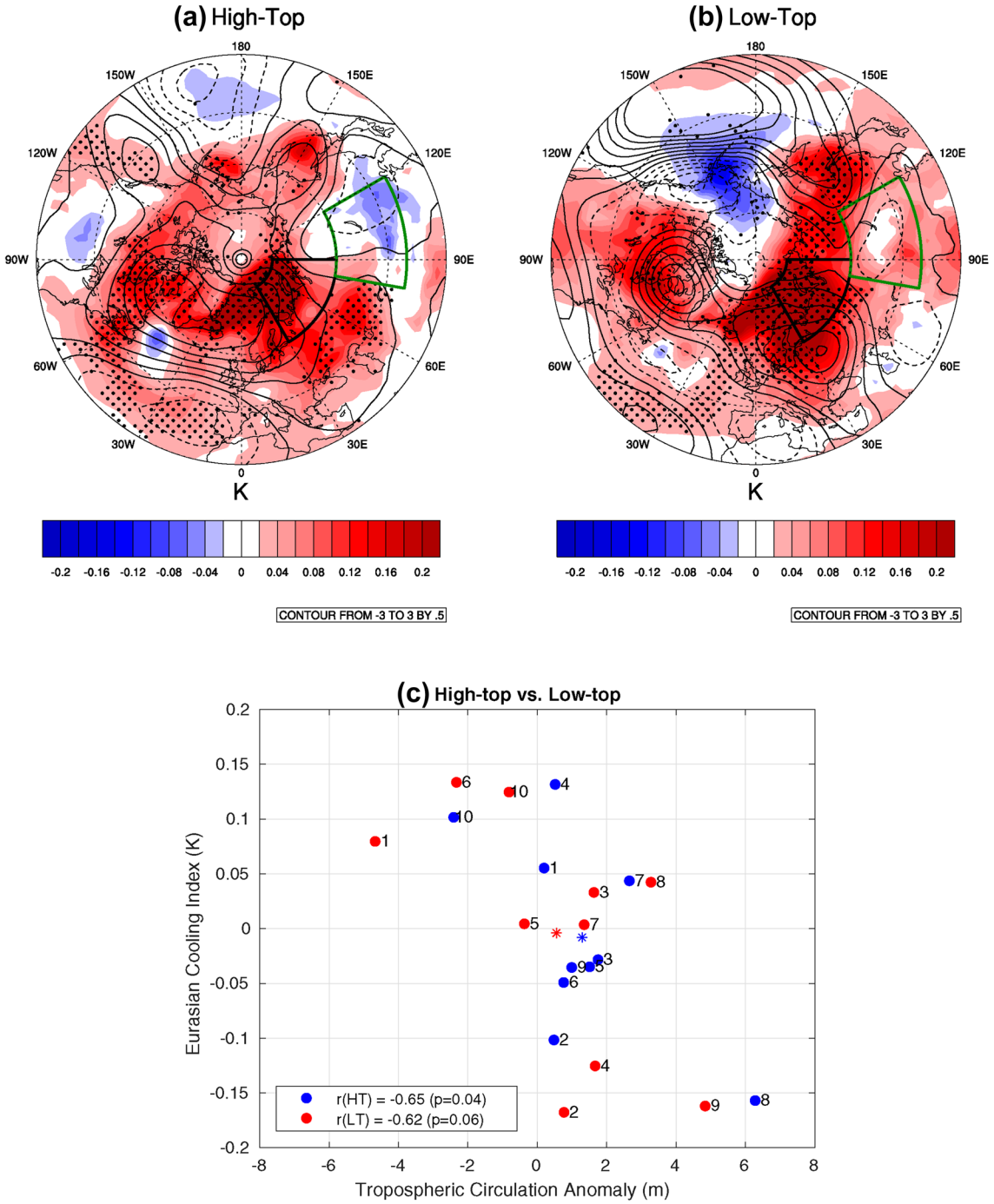

Fig. 6 Similar to Fig. 1 but for surface air temperature (color shadings) and 500 hPa geopotential height (black contours) during February in **a** high-top and **b** low-top models. Positive values in geopotential height are solid while negative values are dashed. Contour interval is 0.5 m. The regions to construct the Ural mountain ridge anomaly and the Eurasia cold anomaly are highlighted in thick black and green boxes, respectively. **c** Scatter plot of 500 hPa geopotential height anomaly over 60°–80°N and 30°–90°E versus Eurasia SAT (ECI) over 40°–60°N and 80°–120°E during February associated with BKS SIC loss in the previous November and December in high-top models (in blue) and low-top models (in red). The numbers represent the corresponding models listed in Tables 1 and 2. The multi-model mean is shown as asterisk in blue for high-top and red for low-top, respectively. The correlation coefficient (r) and p-value are shown in the legend for high-top and low-top models, respectively

specifically, we define the anomalous mid-tropospheric ridge as the weighted area averaged 500 hPa geopotential height anomaly over 60°–80°N 30°–90°E and construct an Eurasian Cooling Index (ECI) as the weighted area averaged SAT anomaly over 40°–60°N and 80°–120°E associated with BKS SIC variability. Although the multi-model mean is not able to simulate Eurasian cooling, there is a statistically significant negative correlation between the tropospheric circulation anomaly and ECI among the models (Fig. 6c), which suggests that the models that simulate a stronger intensified ridge near the Ural Mountains are likely to simulate a stronger Siberian cooling.

One possibility underlying the missing Eurasian cooling may be due to air-sea interaction in the coupled models, where oceanic feedbacks can impact the magnitude of the temperature response (Deser et al. 2015, 2016; McCusker et al. 2016). In a modeling study of Deser et al. (2016), they showed that an elevated global sea surface temperature (SST) associated with sea ice loss warms the troposphere by a combination of local and remote processes, which leads to strong thermodynamically induced warming over the high-latitude continents and dominates over the dynamically induced intensified Siberian high and associated cooling over Eurasia. In particular, Deser et al. (2016) argued that in response to the Arctic sea ice loss, warm SST is confined near the edge of the Arctic in the atmospheric models, whereas the warming spreads to lower latitudes of the ocean basins in the coupled model simulations (note positive SST anomaly over lower latitudes in Fig. 6a, b). Consequently, the dynamically-induced cooling might be weakened or even eliminated by the thermodynamically induced warming (Screen et al. 2018).

Therefore, even though we find robust responses in tropospheric circulation associated with SIC variability via the stratospheric pathway, the resulting surface air temperature anomaly over Eurasia, especially in the coupled model experiments, remains an open question.

4 Conclusion and discussion

Through multi-model analysis of coupled climate models, this study reveals the robustness of the prolonged impact of the stratospheric pathway in linking BKS SIC variability and mid-latitude circulations. In the first part, we find that high-top multi-model mean simulates a stronger circulation response than the low-top counterpart during mid winter associated with fall BKS SIC variability, especially in zonal wind and geopotential height. The results also exhibit that the largest circulation responses are evident over the North Atlantic region and are more persistent in high-top models than low-top. In the second part, we attribute the differences in mid-latitude circulation anomaly between high-top and low-top models to the representation of the stratospheric pathway. Compared to low-top models, we find a stronger and longer-lived negative NAM-like pattern in high-top models. During upward propagation phase, a stronger vertical wave propagation is found in high-top models, which leads to a stronger weakening of the stratospheric polar vortex. In particular, we show that the wave-2 eddy heat flux plays the dominant role for the enhanced upward wave propagation following constructive linear interference in high-top models. During downward migration phase, on the other hand, the phase-tilt of wave-1 geopotential height supports the stratosphere-troposphere coupling in high-top models. However, the multi-model mean in neither high-top or low-top is capable of simulating the intensified ridge near the Ural Mountains and associated cooling over Eurasia during mid-winter. Alternatively, the warm ocean basins suggest that a thermodynamic effect, due to ocean coupling, may compensate the dynamical cooling in the coupled models.

Previously, only a few studies examined the connection between the Arctic and the mid-latitudes using CMIP5 multi-model ensemble, however, the mechanism remains inconclusive due to the contrasting methodologies and results. For example, Zappa et al. (2018) found the largest mid-latitude circulation response during late winter due to future projected sea ice loss, however, Boland et al. (2017) found no support for a linkage between sea ice and atmospheric circulation in CMIP5 future projections. In contrast to them, our study investigates the impact of Arctic sea ice variability in pre-industrial control experiments, with a particular focus on the comparison between high-top and low-top models. It should also be noted that, in contrast to another study by Kelleher and Screen (2018), we solely examine the impact of BKS SIC variability and do not consider the dynamical mechanisms leading to the SIC variability.

Overall, this multi-model analysis has clearly demonstrated the robustness of the prolonged circulation responses over the mid-latitudes associated with the BKS SIC variability and a critical role of the stratospheric pathway. In particular, our study includes: (1) an assessment of the stratospheric pathway in a multi-model ensemble using diverse models from different modeling groups. (2) a detailed analysis of stratosphere-troposphere coupling which helps to distinguish the dynamics and its impact between high-top and low-top models. More specifically, we explicitly identify the zonal wave-2 eddy heat flux as the key for different dynamical coupling between the two groups of models.

While high-top and low-top multi-model mean shows robust differences in the simulation of tropospheric circulation associated with BKS sea ice variability, there are a few caveats that we should consider. Firstly, the collective performance of the two model groups is not necessarily true when we examine each individual model. Instead, we find a considerable spread in the model response in each

group (Fig. 6c and S3). Secondly, in addition to model lid height, high-top and low-top model groups also have different model physics that could possibly cause the difference and inter-model spread. For example, in an assessment of troposphere-stratosphere coupling in CMIP5 future projections, Manzini et al. (2014) argued that the division of high-top and low-top models in future warming scenarios may not be reliable due to inter-model difference in climate sensitivity. Therefore, to unambiguously distinguish the role of the stratospheric pathway, "nudging" might be a better methodology. But previous studies using nudging method (e.g. Nakamura et al. 2016; Wu and Smith 2016; Zhang et al. 2017) have found consistent conclusions that troposphere-stratosphere coupling is largely responsible for the prolonged tropospheric circulation response. The third point concerns that using daily variables instead of monthly may be a better way to assess the chain of events involving the troposphere-stratosphere coupling, especially for identifying peak eddy heat flux and following stratospheric response. Lastly, we acknowledge that correlation does not necessarily imply causation, and the lead-lag regression may not be the best way to identify the consequences of sea ice variability on the mid-latitude circulation response. For example, McGraw and Barnes (2018) used a "Granger Causality" approach to better establish the causality by ensuring that the results are not due to memory in data. Barnes and Simpson (2017) also took "Granger Causality" to quantify the response of zonal wind to variability of Arctic temperature on subseasonal time scale. They found a robust impact but only a small additional percentage of the variance of the jet position and speed can be attributed to Arctic Amplification. In addition, Kretschmer et al. (2016) introduced another novel approach of time series analysis named "Causal Effect Networks" to identify a causal relationship between the BKS SIC and winter circulation in the observations. They found that the autumn BKS SIC is a major driver of mid-latitude winter circulation by influencing the weakened polar vortex and negative NAO pattern.

In summary, our results complement the conclusions of previous studies (Kim et al. 2014; Sun et al. 2015; Nakamura et al. 2016; Wu and Smith 2016; Zhang et al. 2017) and suggests that the stratospheric pathway plays an important role for a persistent and amplified mid-latitude circulation response associated with BKS SIC variability. We explicitly demonstrate that CMIP5 high-top models, collectively, better simulate a stronger vertical wave propagation and long-lasting downward coupling that produces a teleconnection between the Arctic and the mid-latitude via a "stratospheric bridge". This study also suggests possible issues in low-top global climate models, especially for understanding NH weather and climate conditions. The results will be helpful for further improvement of global climate models by incorporating a well-resolved stratosphere.

Acknowledgements We acknowledge the World Climate Research Programmes Working Group on Coupled Modeling for CMIP and we thank each climate modeling groups for producing and making available the model output. De and Wu were supported by National Science Foundation under grant NSF AGS-1406962 and Purdue University to conduct this research. We thank Lantao Sun for constructive discussion at early stage of this study. We are thankful to Paul Kushner and Chaim Garfinkel for important comments. We thank NCAR and participating scientists for a constructive workshop on CMIP analysis platform with a particular focus on multi-model ensemble analysis. We also thank Wen-wen Tung and Pengfei Zhang for useful discussion. We acknowledge the computing resources at Purdue University. Lastly, we are thankful to two anonymous reviewers for their insightful suggestions to improve the manuscript.

References

Bader J, Mesquita MDS, Hodges KI, Keenlyside N, sterhus S, Miles M (2011) A review on northern hemisphere sea–ice, storminess and the North Atlantic oscillation: observations and projected changes. Atmos Res 101:809–834. https://doi.org/10.1016/j.atmosres.2011.04.007

Barnes EA, Screen JA (2015) The impact of Arctic warming on the midlatitude jet-stream: can it? Has it? Will it? Wiley Interdiscip Rev Clim Change 6(3):277–286. https://doi.org/10.1002/wcc.337

Barnes EA, Simpson IR (2017) Seasonal sensitivity of the northern hemisphere jet-streams to Arctic temperatures on subseasonal timescales. J Clim 30(24):10,117–10,137. https://doi.org/10.1175/JCLI-D-17-0299.1

Boland EJD, Bracegirdle TJ, Shuckburgh EF (2017) Assessment of sea ice-atmosphere links in CMIP5 models. Clim Dyn 49:683–702. https://doi.org/10.1007/s00382-016-3367-1

Cai D, Dameris M, Garny H, Runde T (2012) Implications of all season arctic sea–ice anomalies on the stratosphere. Atmos Chem Phys 12:11,819–11,831. https://doi.org/10.5194/acp-12-11819-2012

Cassano EN, Cassano JJ, Higgins ME, Serreze MC (2014) Atmospheric impacts of an arctic sea ice minimum as seen in the community atmosphere model. Int J Climatol 34:766–779. https://doi.org/10.1002/joc.3723

Charlton-Perez AJ, Baldwin MP, Birner T, Black RX, Butler AH, Calvo N, Davis NA, Gerber EP, Gillett N, Hardiman S, Kim J, Krger K, Lee Y, Manzini E, McDaniel BA, Polvani L, Reichler T, Shaw TA, Sigmond M, Son S, Toohey M, Wilcox L, Yoden S, Christiansen B, Lott F, Shindell D, Yukimoto S, Watanabe S (2013) On the lack of stratospheric dynamical variability in low-top versions of the CMIP5 Models. J Geophys Res Atmos 118:2494–2505. https://doi.org/10.1002/jgrd.50125

Charney JG, Drazin PG (1961) Propagation of planetary-scale disturbances from the lower into the upper atmosphere. J of Geophys Res 66:83–109. https://doi.org/10.1029/JZ066i001p00083

Cohen J, Foster J, MBarlow, Saito K, Jones J (2010) Winter 2009–2010: a case study of an extreme Arctic oscillation event. Geophys Res Lett 37(L17):707. https://doi.org/10.1029/2010GL044256

Cohen J, Screen JA, Furtado JC, Barlow M, Whittleston D, Coumou D, Francis J, Dethloff K, Entekhabi D, Overland J, Jones J (2014) Recent Arctic amplification and extreme mid-latitude weather. Nat Geosci 7:627–637. https://doi.org/10.1038/ngeo2234

Collins M et al (2013) Long-term climate change: projections, commitments and irreversibility. Clim Change Phys Sci Basis 1029 –1136

Comiso JC (2000) bootstrap sea ice concentrations from nimbus-7 SMMR and DMSP SSM/I-SSMIS, Version 2, [1979-2013]. Boulder, Colorado USA NASA DAAC at the National Snow and Ice Data p https://doi.org/10.5067/J6JQLS9EJ5HU

Dee DP, Coauthors (2011) The ERA-interim reanalysis: configuration and performance of the data assimilation system. QJR Meteorol Soc 137:553–597. https://doi.org/10.1002/qj.828

Deser C, Tomas RA, Sun L (2015) The role of oceanatmosphere coupling in the zonal-mean atmospheric response to arctic sea ice loss. J Clim 28:2168–2186. https://doi.org/10.1175/JCLI-D-14-00325.1

Deser C, Sun L, Tomas RA, Screen J (2016) Does ocean coupling matter for the Northern extratropical response to projected Arctic sea ice loss? Geophys Res Lett 43:2149–2157. https://doi.org/10.1002/2016GL067792

Furtado JC, Cohen JL, Butler AH, Riddle EE, Kumar A (2015) Eurasian snow cover variability and links to winter climate in the CMIP5 models. Clim Dyn 45:2591–2605

Garfinkel CI, Hartmann DL, Sassi F (2010) Tropospheric precursors of anomalous northern hemisphere stratospheric polar vortices. J Clim 23:3282–3299. https://doi.org/10.1175/2010JCLI3010.1

Garfinkel CI, Shaw TA, Hartmann DL, Waugh DW (2012) Does the Holton tan mechanism explain how the Quasi-Biennial oscillation modulates the Arctic polar vortex? J Atmos Sci 69:1713–1733. https://doi.org/10.1175/JAS-D-11-0209.1

Gong T, Feldstein S, Lee S (2017) The role of downward infrared radiation in the recent Arctic winter warming trend. J Clim pp 4937–4949. https://doi.org/10.1175/JCLI-D-16-0180.1

Hoshi K, Ukita J, Honda M, Iwamoto K, Nakamura T, Yamazaki K, Dethloff K, Jaiser R, Handorf D (2017) Poleward Eddy heat flux anomalies associated with recent Arctic sea ice loss. Geophys Res Lett 44:446–454. https://doi.org/10.1002/2016GL071893

Jaiser R, Dethloff K, Handor D (2013) Stratospheric response to Arctic sea ice retreat and associated planetary wave propagation changes. Tellus 65A(19):375. https://doi.org/10.3402/tellusa.v65i0.19375

Kelleher M, Screen J (2018) Atmospheric precursors of and response to anomalous Arctic sea ice in CMIP5 models. Adv Atmos Sci 35:27–37. https://doi.org/10.1007/s00376-017-7039-9

Kidston J, Gerber E (2010) Intermodel variability of the poleward shift of the Austral Jet stream in the CMIP3 integrations linked to biases in 20th century climatology. Geophys Res Lett 37(L09):708. https://doi.org/10.1029/2010GL042873

Kim BM, Son SW, Min SK, Jeong JH, Kim SJ, Zhang X, Shim T, Yoon JH (2014) Weakening of the stratospheric polar vortex by Arctic sea ice loss. Nat Commun 5:4646. https://doi.org/10.1038/ncomms5646

Kretschmer M, Coumou D, Donges JF, Runge J (2016) Using causal effect networks to analyze different Arctic drivers of midlatitude winter circulation. J Clim 29:4069–4081. https://doi.org/10.1175/JCLI-D-15-0654.1

Kug JS, Jeong JH, Jang YS, Kim BM, Folland CK, Min SK, Son SW (2015) Two distinct influences of arctic warming on cold winters over North America and East Asia. Nat Geosci 8:759–762. https://doi.org/10.1038/ngeo2517

Lu J, Cai M (2009) Seasonality of polar surface warming amplification in climate simulations. Geophys Res Lett 36(L16):704. https://doi.org/10.1029/2009GL040133

Manzini E, Karpechko AY, Anstey J, Baldwin MP, Black RX, Cagnazzo C, Calvo N, Charlton-Perez A, Christiansen B, Davini P, Gerber E, Giorgetta M, Gray L, Hardiman SC, Lee YY, Marsh DR, McDaniel BA, Purich A, Scaife AA, Shindell D, Son SW, Watanabe S, Zappa G (2014) Northern winter climate change: assessment of uncertainty in CMIP5 projections related to stratosphere-troposphere coupling. J Geophys Res Atmos 119:7979–7998. https://doi.org/10.1002/2013JD021403

McCusker KE, Fyfe JC, MS M (2016) Twenty-five winters of unexpected Eurasian cooling unlikely due to Arctic sea–ice loss. Nat Geosci 9:838–842. https://doi.org/10.1038/ngeo2820

McGraw M, Barnes EA (2018) Memory matters: a case for granger causality in climate variability studies. J Clim. https://doi.org/10.1175/JCLI-D-17-0334.1

Mori M, Watanabe M, Shiogama H, Inoue J, Kimoto M (2014) Robust arctic sea–ice influence on the frequent eurasian cold winters in past decades. Nat Geosci 7:869–873. https://doi.org/10.1038/ngeo2277

Nakamura T, Yamazaki K, Iwamoto K, Honda M, Miyoshi Y, Ogawa Y, Tomikawa Y, Ukita J (2016) The stratospheric pathway for Arctic impacts on midlatitude climate. Geophys Res Lett 43:3494–3501. https://doi.org/10.1002/2016GL068330

Overland JE, Wood KR, Wang M (2011) Warm Arctic-cold continents: climate impacts of the newly open Arctic Sea. Polar Res 30(1):15,787. https://doi.org/10.3402/polar.v30i0.15787

Pithan F, Mauritsen T (2014) Arctic amplification dominated by temperature feedbacks in contemporary climate models. Nat Geosci 7:181–184. https://doi.org/10.1038/ngeo2071

Polvani LM, Waugh D (2004) Upward Wave Activity Flux as Precursor to Extreme Stratospheric Events and Subsequent Anomalous Surface Weather Regimes. J Clim 17:3548–3554, https://doi.org/10.1175/1520-0442(2004)017<3548:UWAFAA>2.0.CO;2

Sassi F, Garcia RR, Marsh D, Hoppel KW (2010) The role of the middle atmosphere in simulations of the troposphere during Northern Hemisphere winter: differences between high- and low-top models. J Atmos Sci 67:3048–3064. https://doi.org/10.1175/2010JAS3255.1

Screen JA (2017) Simulated atmospheric response to regional and Pan-Arctic sea ice loss. J Clim 30:3945–3962. https://doi.org/10.1175/JCLI-D-16-0197.1

Screen JA, Simmonds I (2010) The central role of diminishing sea ice in recent Arctic temperature amplification. Nature 464:1334–1337. https://doi.org/10.1038/nature09051

Screen JA, Simmonds I, Deser C, Tomas R (2013) The atmospheric response to three decades of observed Arctic sea ice loss. J Clim 26:1230–1248. https://doi.org/10.1175/JCLI-D-12-00063.1

Screen JA, Deser C, Simmonds I, Tomas R (2014) Atmospheric impacts of Arctic sea–ice loss, 1979–2009: separating forced change from atmospheric internal variability. Clim Dyn 43:333–344. https://doi.org/10.1007/s00382-013-1830-9

Screen JA, Deser C, Smith D, Zhang X, Blackport R, Kushner PJ, Oudar T, McCusker K, Sun L (2018) Consistency and discrepancy in the atmospheric response to Arctic sea–ice loss across climate models. Nat Geosci 11:155–163. https://doi.org/10.1038/s41561-018-0059-y

Shaw TA, Perlwitz J (2010) The impact of stratospheric model configuration on planetary-scale waves in Northern Hemisphere winter. J Clim 23:3369–3389. https://doi.org/10.1175/2010JCLI3438.1

Shaw TA, Perlwitz J, Weiner O (2014) Troposphere–stratosphere coupling: links to North Atlantic weather and climate, including their representation in CMIP5 models. J Geophys Res Atmos 119:5864–5880. https://doi.org/10.1002/2013JD021191

Shepherd TG (2016) Effects of a warming Arctic. Science 353:989–990. https://doi.org/10.1126/science.aag2349

Simpson IR, Blackburn M, Haigh JD (2009) The role of eddies in driving the tropospheric response to stratospheric heating perturbations. J Atmos Sci 66:1347–1365. https://doi.org/10.1175/2008JAS2758.1

Smith KL, Fletcher CG, Kushner PJ (2010) The role of linear interference in the annular mode response to extratropical surface forcings. J Clim 23:6036–6050. https://doi.org/10.1175/2010JCLI3606.1

Strey ST, Sara T, Chapman WL, Walsh JE (2010) The 2007 sea ice minimum: impacts on the Northern hemisphere atmosphere in

late autumn and early winter. J Geophys Res 115(D23):103. https://doi.org/10.1029/2009JD013294

Sun L, Deser C, Tomas R (2015) Mechanisms of stratospheric and tropospheric circulation response to projected Arctic sea ice loss. J Clim 28:7824–7845. https://doi.org/10.1175/JCLI-D-15-0169.1

Taylor KE, Stouffer R, Meehl G (2012) An overview of CMIP5 and the experiment design. Bull Am Meteorol Soc 93:485–498

Vihma T (2014) Effects of arctic sea ice decline on weather and climate: a review. Surv Geophys 35:1175–1214. https://doi.org/10.1007/s10712-014-9284-0

Wu Q, Zhang X (2010) Observed forcing-feedback processes between northern hemisphere atmospheric circulation and Arctic sea ice coverage. J Geophys Res Atmos 115(D14):119. https://doi.org/10.1029/2009JD013574

Wu Y, Smith KL (2016) Response of Northern hemisphere midlatitude circulation to Arctic amplification in a simple atmospheric general circulation model. J Clim 29:2041–2058. https://doi.org/10.1175/JCLI-D-15-0602.1

Yang XY, Yuan X, Ting M (2016) Dynamical link between the Barents-Kara sea ice and the Arctic oscillation. J Clim 29:5103–5122. https://doi.org/10.1175/JCLI-D-15-0669.1

Zappa G, Pithan F, Shepherd TG (2018) Multimodel evidence for an atmospheric circulation response to Arctic sea ice loss in the CMIP5 future projections. Geophys Res Lett 45:1011–1019. https://doi.org/10.1002/2017GL076096

Zhang P, Wu Y, Smith KL (2017) Barents kara sea sea ice variability to the midlatitude circulation in a simplified model. Clim Dyn 1–13. https://doi.org/10.1007/s00382-017-3624-y

Zhang P, Wu Y, Simpson IR, Smith KL, Zhang X, De B, Callaghan P (2018) A stratospheric pathway linking a colder siberia to barents-kara sea ice loss. Science Advances 4, https://doi.org/10.1126/sciadv.aat6025